

## Transformation of Binomial Input by the Postsynaptic Membrane at a Central Synapse

**Abstract.** Although a binomial model gives an adequate description of the release properties of central afferent synapses, slight differences between experimental and predicted probability density functions are observed, with an excess number of responses recorded around the means. These discrepancies can be quantified by comparing experimental and theoretical entropies, which could relate to information transfer at these junctions. A model, based on the experimentally supported assumption that the postsynaptic membrane functions as a nonlinear processor, minimizes the differences between the distributions of the recorded and predicted potentials. According to this model, the nonlinearity is due to a localized interaction between the effects of simultaneously activated adjacent synapses.

On the assumption that at chemically mediating junctions the number of quanta released per impulse is binomially distributed, the number of quanta released is determined by the number of units undergoing exocytosis,  $n$ , and the release probability of one unit,  $p$ , which are purely presynaptic variables (1). This fundamental concept is based on two principles: (i) that release at a given active zone is a random process, independent of exocytosis at the other release sites and (ii) that the postsynaptic potentials (PSP's) or currents classically used to estimate  $n$  and  $p$  (1) are mirror images of the release phenomena. We now present evidence suggesting that such is not the case at central synapses and that information carried by the input can be reorganized by the postsynaptic side of the junction.

Data were obtained at inhibitory synapses of the goldfish (*Carassius auratus*) Mauthner (M) cell, through the use of a technique (2, 3) illustrated in Fig. 1A. Fluctuating inhibitory postsynaptic potentials (IPSP's) were evoked by presynaptic impulses (Fig. 1B). A computational procedure gave the optimum fits of the data according to a simple binomial model, under the assumption that  $p$  and the quantal size  $q$  are equal at all terminals.

Figure 2A is similar to those which earlier showed that binomial predictions provide a satisfactory definition of IPSP amplitude fluctuations and that the derived value of  $n$  equals the number of presynaptic active zones (2-4). The optimum values of binomial  $p$  and  $n$  were 0.45 and 13, respectively, and the total number of synaptic boutons stained with horseradish peroxidase (HRP) that were established on the M cell by this presynaptic neuron was also 13 (Fig. 3A).

Statistical tests usually indicated (2, 3) that the data fit the theoretical model. However, a closer inspection of the probability density functions (PDF's) showed that they were systematically biased, with fewer unitary IPSP's in the extreme values than expected from the

binomial predictions and with an excess of responses around the means (Fig. 2A); these differences are also apparent in cumulative distributions (Fig. 2B).

Discrepancies between the recorded and predicted PDF's were quantified with the entropies of their underlying random variables used as an index. Specifically, if  $X$  is a discrete random variable with a set of  $t$  possible values associated with the probabilities  $p_i$ , where  $i = 1, \dots, t$ , the entropy of  $X$ , which is a measure of the uncertainty of the estimate of  $X$  resulting from a random sampling experiment (5), can be defined by

$$E_x = - \sum_{i=1}^t p_i \log p_i$$

This relation was used to determine the entropies of the experimental results  $E_{\text{exp}}$ , and of the binomial predictions  $E_{\text{th}}$ , through the use of an adapted discretization scheme (6), and a variable

$$\Delta E = 100(E_{\text{th}} - E_{\text{exp}})/E_{\text{th}}$$

was defined. At low frequencies of stimulations (up to 10 Hz),  $\Delta E$  ranged from 0.4 to 21.76 with a mean of 11.27 [standard deviation (S.D.) = 4.74,  $n = 35$ ],

$E_{\text{exp}}$  thus being consistently smaller than  $E_{\text{th}}$ . These findings suggest the existence of a synaptic mechanism through which the postsynaptic responses are grouped and which is more organized than predicted by the binomial relation.

A simple binomial description of release remains appropriate since (i) it has generated a powerful structure-function correlation and (ii) tests with a nonuniform (compound) binomial model with various values of  $p$  at each terminal [7; see also (1)], were performed: better fits, if any, were then obtained at the expense of this correlation. Also, presynaptic values did not affect  $\Delta E$ . In cases of cells with terminals restricted within the axon cap,  $\Delta E$  still averaged 10.34 (S.D. = 4.78;  $n = 8$ ). Variations of  $p$  did not significantly affect mean  $\Delta E$ , which was 10.52 (S.D. = 4.93;  $n = 17$ ) and 11.98 (S.D. = 4.58;  $n = 18$ ) in series in which  $p$  ranged from 0.20 to 0.40 and from 0.41 to 0.75, respectively. Similarly, when values of  $n$  were grouped in three classes (of 3 to 10, 11 to 20, and 21 to 63 boutons),  $\Delta E$  was constant, averaging 11.53 (S.D. = 5.89;  $n = 15$ ), 11.38 (S.D. = 4.66;  $n = 13$ ), and 11.09 (S.D. = 3.55;  $n = 7$ ).

Data suggesting that the grouping of evoked responses was of postsynaptic origin were obtained with a competitive blocker of glycine, the putative transmitter at these junctions (8). In a first series ( $n = 5$ ), strychnine was applied iontophoretically to the M cell's soma through a third microelectrode;  $\Delta E$  decreased by 0.55 to 19.5, with an average reduction of 9.77 [S.D. = 6.87; paired  $t$ -tests,  $P < 0.025$ ]. In these cases,  $p$  and  $n$  remained unaffected (9), which confirms a postsynaptic drug action. In a second group ( $n = 8$ ), the blocker was adminis-

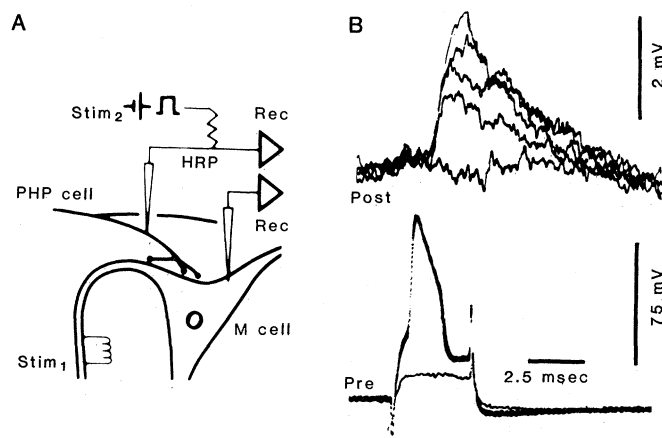


Fig. 1. Quantal fluctuations of unitary IPSP's. (A) Diagram of experiment for simultaneous intracellular recording (Rec) from the M cell and a presynaptic interneuron (PHP cell), both identified by their responses to antidromic stimulation ( $\text{Stim}_1$ ). The postsynaptic electrode was filled with KCl, so that inhibitory potentials were depolarizing, and the presynaptic electrode was used

for intracellular stimulation ( $\text{Stim}_2$ ) and subsequent iontophoretic injections of HRP for histological reconstruction of the stained interneurons. (B) Unitary IPSP's of variable amplitudes (upper traces) produced in the M cell by single impulses directly evoked in the presynaptic neuron (lower traces). Stimulus current (not shown) straddled threshold for spike initiation. The same experiment is shown in Figs. 2 and 3.

tered intramuscularly, and  $\Delta E$  was unusually low, with a mean of  $1.67 \pm 0.40$  (range, 1.15 to 2.31).

These data led us to reexamine the notion (3, 10) that postsynaptic conductance changes at adjacent synaptic loci are independent and directly proportional to the number of releasing terminals. We derived a postsynaptic transfer function relating the amount of transmitter released to the resultant conductance change, such that the theoretical PDF was transformed to the experimental one. This function was computed on the basis of  $f$ , the estimated (binomial) PDF of the release process, and  $\varphi$ , that of the recorded potentials.  $\varphi$  represents the output variable, that is, the conductance increments due to transmitter action;  $f$  corresponds to the input variable, namely, the amount of transmitter released after each impulse, expressed in quantal units. We found (11) that this transform is unique, and it is defined by  $r = \Phi^{-1} \circ F$  where  $F$  and  $\Phi$  are the cumulative functions associated with  $f$  and  $\varphi$ , respectively, and  $\circ$  stands for composition of functions.

Figure 3B is typical of the transforms so obtained. The amplitude of the response to several quanta is less than that

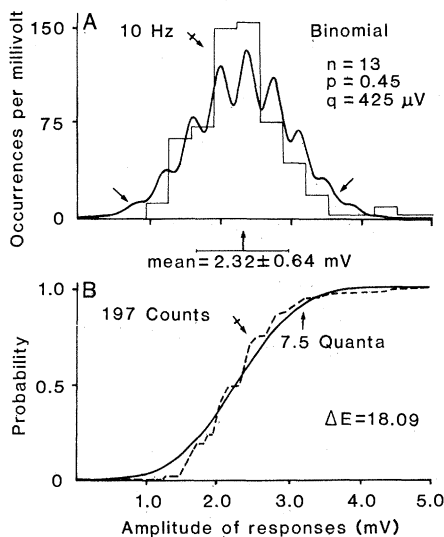


Fig. 2. Enhancement of postsynaptic response frequencies within the range of their predicted mean amplitude. (A) Probability density function (stepwise distribution for 197 counts) of unitary IPSP fluctuations (thin lines) and computer-modeled best fit (binomial model, thick line). The stimulus was 10 Hz. The Kolmogorov test was poorly satisfied ( $P < 0.040$ ) and the number of recorded PSP's was less than that predicted at the extremes of the spectrum (arrows). By contrast, they were in excess around the mean (crossed arrow). (B) Cumulative probability functions of the predicted IPSP amplitudes (thick line) and of the potentials recorded in the M cell (dashed line).  $E_{th}$  was less than  $E_{exp}$ ;  $\Delta E = +18.09$  (arrow as in Fig. 3B).

predicted by the proportionality assumption. Thus, the postsynaptic membrane adds quantal conductances nonlinearly. The magnitude of the nonlinearities of the transfer function  $r$  depended largely on the grouping of the presynaptic terminals in distinct clusters. For instance, the five cells with the lowest  $\Delta E$ 's, ranging from 0.4 to 5.31 ( $\bar{X} = 3.04$ , S.D. = 2.42), were morphologically exceptional since their terminals were separated considerably (no less than  $30 \mu\text{m}$ ). Thus,  $r$  presumably reflects the degree of a spatially restricted postsynaptic interaction with a progressive decrease in the mean response per bouton when several terminals are activated simultaneously.

This possibility (Fig. 3C) was modeled by computer. The program, based on the geometrical characteristics of the reconstructed presynaptic neurons, distinguished two classes: (i) terminals, which are clustered within a radius up to  $20 \mu\text{m}$  and release independently but have intersecting zones of influence, such that response increment per activated knob is less than the quantal size (for a first approximation the magnitude of interaction was constant throughout the cluster, varying only with the number of activated terminals); and (ii) isolated boutons. The simulation procedure computed the distribution of responses generated according to the derived binomial parameter  $p$  and the modeled interaction within the clusters. Finally, a theoretical transfer function similar to  $r$  was derived. For instance, the histological reconstruction of the neuron of Fig. 3A showed two widely disposed clusters of eight and five terminal boutons. The program used the transmitter-response relationship (Fig. 3D) for both clusters. In this and other experiments, the theoretical function  $r$  satisfactorily fit its experimental counterpart (Fig. 3B).

The transfer function that eliminates the discrepancies between experimental and theoretical PDF's can be simulated by modeling nonlinear increments in quantal conductances, restricted to the effects of simultaneously activated closely located terminals. The basis for such a postsynaptic interaction is unclear: properties of M cell responses suggest that voltage dependence of quantal PSP's or transient increased local conductances (12) are unlikely (2, 3, 13). The effects produced by release at each synaptic bouton may be due to a diffuse action of the transmitter over domains larger than those restricted under a given release site (14), or alternatively, the synaptic current produced at clustered junctions may be saturated, for example, by local ionic movements and shifts in the IPSP

driving force. In the latter case, the reduction in quantal size after strychnine administration would then minimize the nonlinearities.

In terms of information processing, the individual active zone or release site remains the quantal or functional unit, but the postsynaptic membrane seems to favor the occurrence of the responses close to the mean and to minimize their randomness. This peculiar filtering procedure may be significant in terms of stabilizing the sensory input in a highly integrative and command neuron (15).

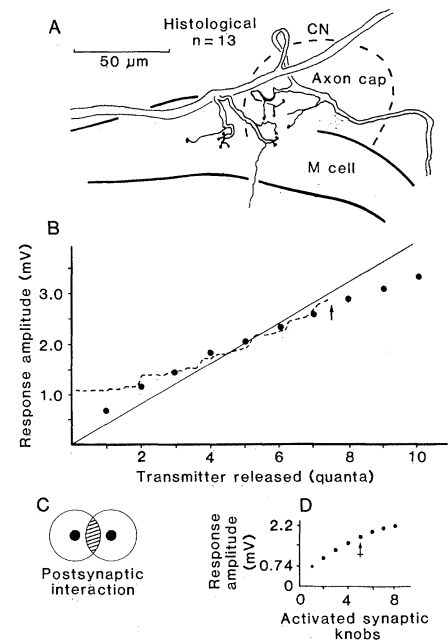


Fig. 3. Evidence for localized interaction between the effects of adjacent synapses. (A) Camera-lucida reconstruction of the HRP-filled commissural interneuron (CN) that evoked the responses used for Figs. 1 and 2. (B) Relationship between the amount of transmitter released and the amplitudes of the postsynaptic responses. Solid line, linear relationship that would pertain if the responses were directly proportional to transmitter output. Dashed line, calculated function  $r$ , which, if applied to the theoretical PDF, would produce conductance changes similar to those accompanying the recorded IPSP's over the range of reliability, that is, to 7.5 quanta (arrow). The marked deviation of this curve from the solid line suggests a localized interaction between synaptic effects when several terminals are simultaneously active. Dots, computer-modeled  $r$  function. (C) Proposed interactions occurring when two synapses (black circles) of a cluster are simultaneously active, and their zones of influence (large circles) overlap (hatched area). (D) Modeled relationship between response amplitude and the number of activated synaptic knobs. These amplitudes, normalized to equate the mean binomial response with that obtained after transform, were 0.74, 1.03, 1.29, 1.55, 1.77, 1.96, 2.11 and 2.22 mV, respectively, as one to eight synapses were active. The crossed arrow indicates the maximum response produced by the second cluster of five terminals.

Nonlinear summation of the effects of clustered terminals could also account for the lack of fits observed in other preparations, including when analyzing fluctuating PSP's evoked in motoneurons by Ia synapses [7; see also (1)].

HENRI KORN

Département de Biologie Moléculaire,  
INSERM U261, Institut Pasteur,  
25 Rue du Docteur Roux  
75724 Paris Cedex 15, France

ALAIN MALLET

Département de Biomathématiques,  
INSERM U194,  
CHU Pitié-Salpêtrière,  
75634 Paris Cedex 13, France

#### References and Notes

1. Reviewed in E. M. Mc Lachlan, *Int. Rev. Physiol.* **17**, 49 (1978).
2. H. Korn, A. Triller, A. Mallet, D. S. Faber, *Science* **213**, 899 (1981).
3. H. Korn, A. Mallet, A. Triller, D. S. Faber, *J. Neurophysiol.* **48**, 679 (1982).
4. A. Triller and H. Korn, *ibid.*, p. 708.
5. C. E. Shannon, *Bell Syst. Techn. J.* **27**, 379 (1948); *ibid.*, p. 623; S. Kullback, in *Information Theory and Statistics* (Wiley, New York, 1959).
6. The potential values were allocated into  $n + 2$  classes (where  $n$  is the binomial parameter) with ranges equal to the quantum size  $q$ . Let  $D_i$ ,  $i = 1, \dots, n + 2$  be the  $n + 2$  intervals covering  $R$  (the real numbers) defined as:

$$D_1 = (-\infty, q/2]$$

$$D_i = ((2i - 3)q/2, (2i - 1)q/2],$$

$$i = 2, \dots, n + 1$$

$$D_{n+2} = ((2n + 1)q/2, +\infty)$$

Then the probabilities  $p_i$  were computed as follows:

(i) Predicted probabilities, noted as  $\hat{p}_i$

$$\hat{p}_i = \int_{D_i} f(v) dv$$

(ii) Experimental probabilities

$$p_i = \frac{1}{S} \sum_{j=1}^s 1_{D_i}(v_j)$$

where  $v$  is the recorded potential and  $s$  is the number of stimulations, the corresponding (PSP's) recordings being  $v_j$ , for  $j = 1, \dots, s$ . Then

$$E_{\text{exp}} = - \sum_{i=1}^{n+2} \hat{p}_i \log \hat{p}_i$$

$$E_{\text{th}} = - \sum_{i=1}^{n+2} p_i \log p_i$$

The discrepancies between the distributions were quantified as  $100(E_{\text{th}} - E_{\text{exp}})/E_{\text{th}}$ , to allow comparisons between experiments.

7. T. H. Brown, D. H. Perkel, M. W. Feldman, *Proc. Natl. Acad. Sci. U.S.A.* **73**, 2913 (1976); S. B. Barton and I. S. Cohen, *Nature (London)* **268**, 267 (1976); J. J. B. Jack, S. J. Redman, K. Wong, *J. Physiol. (London)* **321**, 65 (1981)
8. S. Roper, J. Diamond, G. M. Yasargil, *Nature (London)* **223**, 1168 (1969); J. Diamond, S. Roper, G. M. Yasargil, *J. Physiol. (London)* **232**, 87 (1973).
9. D. S. Faber, H. Korn, A. Triller, *Soc. Neurosci. Abstr.* **9**, 456 (1983).
10. D. S. Faber and H. Korn, *J. Neurophysiol.* **48**, 654 (1982).
11. For any amount  $x$  of transmitter released, the probability that  $r(x)$  is less than a given concentration  $y$  must equal the probability that the recorded potential  $v$  is less than the same concentration  $y$ , that is,
 
$$\text{Prob}[r(x) < y] = \text{Prob}[v < y].$$
 As  $r$  is a monotonically increasing function
 
$$\text{Prob}[x < r^{-1}(y)] = \text{Prob}[v < y],$$
 or, with the notation in the text:
 
$$F[r^{-1}(y)] = \Phi[y].$$
 Finally,  $r = \Phi^{-1} \circ F$ , where  $\circ$  stands for composition of functions and  $r^{-1}$  and  $\Phi^{-1}$  express the reciprocals of  $r$  and  $\Phi$ .
12. C. Koch, T. Poggio, V. Torre, *Proc. Natl. Acad. Sci. U.S.A.* **80**, 2799 (1983).
13. T. Furshpan and T. Furukawa, *J. Neurophysiol.* **25**, 732 (1962); Y. Fukami, T. Furukawa, Y. Asada, *J. Gen. Physiol.* **48**, 581 (1965).
14. Cooperation between adjacent synapses has also been described [B. L. Mc Naughton, R. M. Douglas, G. V. Goddard, *Brain Res.* **157**, 277 (1978); H. Korn and D. S. Faber, *Soc. Neurosci. Abstr.* **9**, 456 (1983)].
15. H. B. Barlow, in *Sensory Communication*, W. A. Rosenblith, Ed. (MIT Press, Cambridge, Mass., 1961), p. 217; S. Laughlin, *Z. Naturforsch.*, **36c**, 910 (1981).
16. We thank D. S. Faber and T. Heidmann for helpful comments in interpretation of the data.

30 January 1984; accepted 18 June 1984

gens or  $\gamma$ -radiation (2, 3). The oncogenes that appear to be most frequently activated in humans and in animal model systems belong to the *ras* family: H-, K-, and N-*ras* (4). H- and K-*ras* were first found in rat retroviruses (5). N-*ras* was first found in a human tumor cell line (1), and in other species we found it associated with carcinogen-induced mouse lymphomas (2). All three genes encode closely homologous proteins with a molecular weight of about 21,000 (p21), and each gene, when activated, differs from its normal cellular homolog by a single point mutation that alters the 12th or 61st amino acid of the protein (6).

We recently reported the activation of cellular *ras* (c-*ras*) oncogenes in vivo, in mice treated with a carcinogen or  $\gamma$ -radiation (2). Both treatments cause a high incidence of thymomas in crosses between AKR and RF/J mice, but the carcinogen activates N-*ras* whereas radiation activates K-*ras*. To further characterize the activated K-*ras*, we have studied one of the  $\gamma$ -radiation-induced tumors (tumor X). DNA from tumor X was used to obtain 3T3 primary transformants (Fig. 1A, lane a). With DNA from this primary transformant, secondary transformants were obtained in rat-2 cells (Fig. 1A, lane c) to facilitate the identification and subsequent cloning of mouse sequences (2). The two bands of 17.3 and 14.4 kb on top of lane a represent the endogenous 3T3 band (17.3 kb, compare Fig. 1A, lane e) plus the new information acquired from the tumor (14.4 kb). This band has a different molecular weight because of the rearrangements that frequently occur during gene transfer. If one compares Fig. 1A, lanes a and c, it is clear that only the 14.4-kb band is transferred concordantly with the oncogenic phenotype. Since the point mutations associated with *ras* activation have been found in only two positions, at amino acids 12 and 61 (6), predominantly in the former, we examined the fragment containing the first exon and therefore the sequences for the 12th codon. We found the first exon in the 17.3-kb band in normal mouse DNA and in the 14.4-kb band in the rat transformant by using a specific probe obtained from a Kirsten rat sarcoma virus complementary DNA (cDNA) clone (data not shown) (7). The 17.3-kb band from the mouse brain that developed tumor X and the 14.4-kb from the secondary rat transformant were extracted from agarose gels and shown to be pure (Fig. 1A, lanes f and d). They were subsequently ligated to phage  $\lambda$  47.1 Hind III arms and cloned as described (8).

## Activation of a c-K-*ras* Oncogene by Somatic

### Mutation in Mouse Lymphomas Induced by Gamma Radiation

**Abstract.** *Mouse tumors induced by gamma radiation are a useful model system for oncogenesis. DNA from such tumors contains an activated K-*ras* oncogene that can transform NIH 3T3 cells. This report describes the cloning of a fragment of the mouse K-*ras* oncogene containing the first exon from both a transformant in rat-2 cells and the brain of the same mouse that developed the tumor. Hybrid constructs containing one of the two pieces were made and only the plasmid including the first exon from the transformant gave rise to foci in NIH 3T3 cells. There was only a single base difference (G  $\rightarrow$  A) in the exonic sequence, which changed glycine to aspartic acid in the transformant. By use of a synthetic oligonucleotide the presence of the mutation was demonstrated in the original tumor, ruling out modifications during DNA-mediated gene transfer and indicating that the alteration was present in the thymic lymphoma but absent from other nonmalignant tissue. The results are compatible with gamma radiation being a source of point mutations.*

Certain oncogenes can change the normal morphology of cultured rodent fibroblasts toward an oncogenic phenotype, enabling those that carry the genes to grow in soft agar and form tumors when

injected into nude mice (1). Such oncogenes have been found in human tumors and cell lines derived from them (1) and, more recently, in model systems in which tumors were induced by carcino-